Article

Cell Host & Microbe

Influenza Virus Adaptation PB2-627K Modulates Nucleocapsid Inhibition by the Pathogen Sensor RIG-I

Graphical Abstract

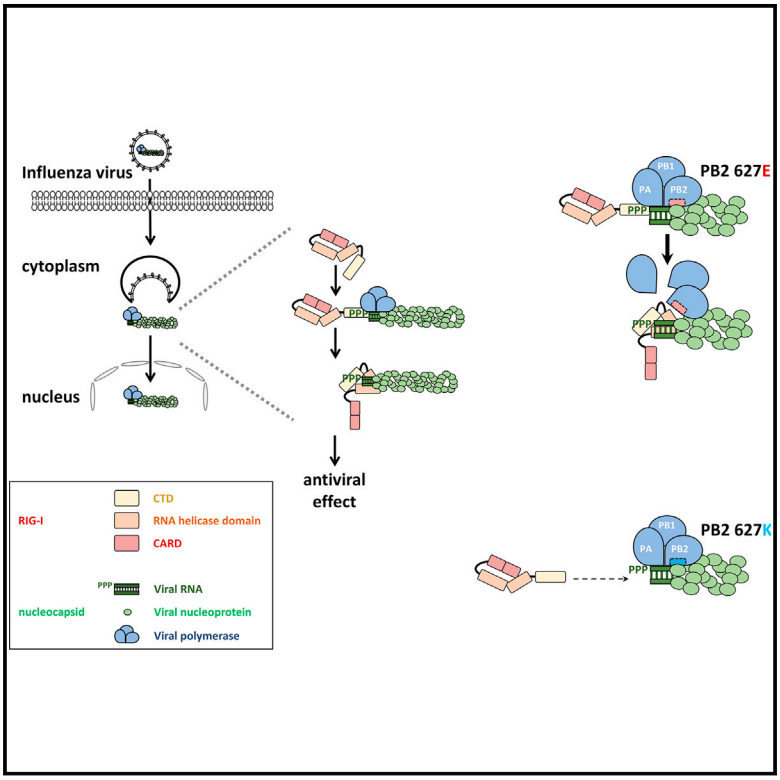

Authors

Michaela Weber, Hanna Sediri, ..., Hans-Dieter Klenk, Friedemann Weber

Correspondence

friedemann.weber@staff.uni-marburg.de

In Brief

RIG-I is a cytoplasmic pathogen recognition receptor that recognizes 5′ppp-dsRNA. Weber et al. show that RIG-I binds the "panhandle" promoter of incoming influenza A viruses and directly inhibits the onset of infection by destabilizing nucleocapsids. Strains with the mammalian-adapted polymerase subunit PB2-627K are more RIG-I resistant than those with avian-adapted PB2-627E.

Highlights

- 5′ppp dsRNA panhandle of incoming influenza virus nucleocapsids activates RIG-I
- Human-adaptive mutation PB2-627K in the viral polymerase counteracts activation of RIG-I
- RIG-I directly inhibits incoming nucleocapsids with the avian PB2-627E signature
- Strength of polymerase binding to nucleocapsids determines RIG-I sensitivity

Weber et al., 2015, Cell Host & Microbe *17*, 309–319
March 11, 2015
http://dx.doi.org/10.1016/j.chom.2015.01.005

Cell Host & Microbe
Article

Influenza Virus Adaptation PB2-627K Modulates Nucleocapsid Inhibition by the Pathogen Sensor RIG-I

Michaela Weber,[1] Hanna Sediri,[1] Ulrike Felgenhauer,[1] Ina Binzen,[1] Sebastian Bänfer,[2] Ralf Jacob,[2] Linda Brunotte,[3] Adolfo García-Sastre,[4,5,6] Jonathan L. Schmid-Burgk,[7] Tobias Schmidt,[7] Veit Hornung,[7] Georg Kochs,[3] Martin Schwemmle,[3] Hans-Dieter Klenk,[1] and Friedemann Weber[1,*]
[1]Institute for Virology
[2]Department of Cell Biology and Cell Pathology
Philipps-University Marburg, D-35043 Marburg, Germany
[3]Institute for Virology, University Medical Center, D-79008 Freiburg, Germany
[4]Department of Microbiology
[5]Department of Medicine, Division of Infectious Diseases
[6]Global Health and Emerging Pathogens Institute
Icahn School of Medicine at Mount Sinai, New York, NY 10029, USA
[7]Institute of Molecular Medicine, University Hospital, University of Bonn, D-53127 Bonn, Germany
*Correspondence: friedemann.weber@staff.uni-marburg.de
http://dx.doi.org/10.1016/j.chom.2015.01.005

SUMMARY

The cytoplasmic RNA helicase RIG-I mediates innate sensing of RNA viruses. The genomes of influenza A virus (FLUAV) are encapsidated by the nucleoprotein and associated with RNA polymerase, posing potential barriers to RIG-I sensing. We show that RIG-I recognizes the 5′-triphosphorylated dsRNA on FLUAV nucleocapsids but that polymorphisms at position 627 of the viral polymerase subunit PB2 modulate RIG-I sensing. Compared to mammalian-adapted PB2-627K, avian FLUAV nucleocapsids possessing PB2-627E are prone to increased RIG-I recognition, and RIG-I-deficiency partially restores PB2-627E virus infection of mammalian cells. Heightened RIG-I sensing of PB2-627E nucleocapsids correlates with previously established lower affinity of 627E-containing PB2 for nucleoprotein and is increased by further nucleocapsid instability. The effect of RIG-I on PB2-627E nucleocapsids is independent of antiviral signaling, suggesting that RIG-I-nucleocapsid binding alone can inhibit infection. These results indicate that RIG-I is a direct avian FLUAV restriction factor and highlight nucleocapsid disruption as an antiviral strategy.

INTRODUCTION

Influenza A viruses (FLUAV; family *Orthomyxoviridae*) are a significant health threat. Regular, global outbreaks are occurring due to replenishment from a seemingly unlimited reservoir of strains in birds (Cauldwell et al., 2014; Klenk, 2014; Mänz et al., 2013). FLUAV virions consist of a lipid envelope with the glycoproteins HA and NA, which also provide the basis for taxonomic classification, as well as the proton channel M2. The inner leaflet of the viral envelope is covered by the M1 protein. Inside the particles are eight nucleocapsids containing the negative-strand RNA genome encapsidated by the nucleoprotein (NP) and associated with the RNA polymerase complex with subunits PB1, PB2, and PA. The eight genome segments encode the main structural proteins, auxiliary proteins (NS1 and NEP) and sometimes other, strain-dependent, factors. Gene expression is regulated by partially complementary 5′ and 3′ end sequences (the ''panhandle'') that pseudocircularize the single-stranded RNA genome and serve as promoter for transcription and replication. An outstanding feature of FLUAV is that most parts of the replication cycle occur in the nucleus.

Retinoic acid-inducible gene I (RIG-I) is an RNA helicase that acts as a major host sensor for virus infections in the cytoplasm (Yoo et al., 2014). RIG-I recognizes nonself RNA structures and activates a signaling cascade leading to phosphorylation of transcription factor IRF3 and induction of the antiviral type I interferons (IFN-α/β).

RIG-I contains a central multipartite helicase/ATPase domain flanked by N-terminal caspase recruitment domains (CARDs) and a C-terminal domain (CTD) (Yoo et al., 2014). Unstimulated RIG-I is in an autorepressed, monomeric conformation with the CARDs confined and the CTD exposed. When the CTD binds a ligand RNA, RIG-I undergoes a conformational switch, enabling it to expose the CARDs for interaction with TRIM25 and MAVS to initiate antiviral signaling (Gack, 2014; Kowalinski et al., 2011; Rawling and Pyle, 2014).

Synthetic short 5′ppp-dsRNA represents the optimal RIG-I ligand (Schlee et al., 2009; Schmidt et al., 2009), a structure with remarkable similarity to the panhandle formed by the annealed 5′ and 3′ genome ends of segmented negative-strand RNA viruses (Schlee, 2013; Weber and Weber, 2014b). Accordingly, naked genomic RNA of FLUAV and other negative-strand RNA viruses is an excellent activator of RIG-I (Habjan et al., 2008; Hornung et al., 2006; Pichlmair et al., 2006). We recently reported that RIG-I is capable of recognizing 5′ppp-dsRNA

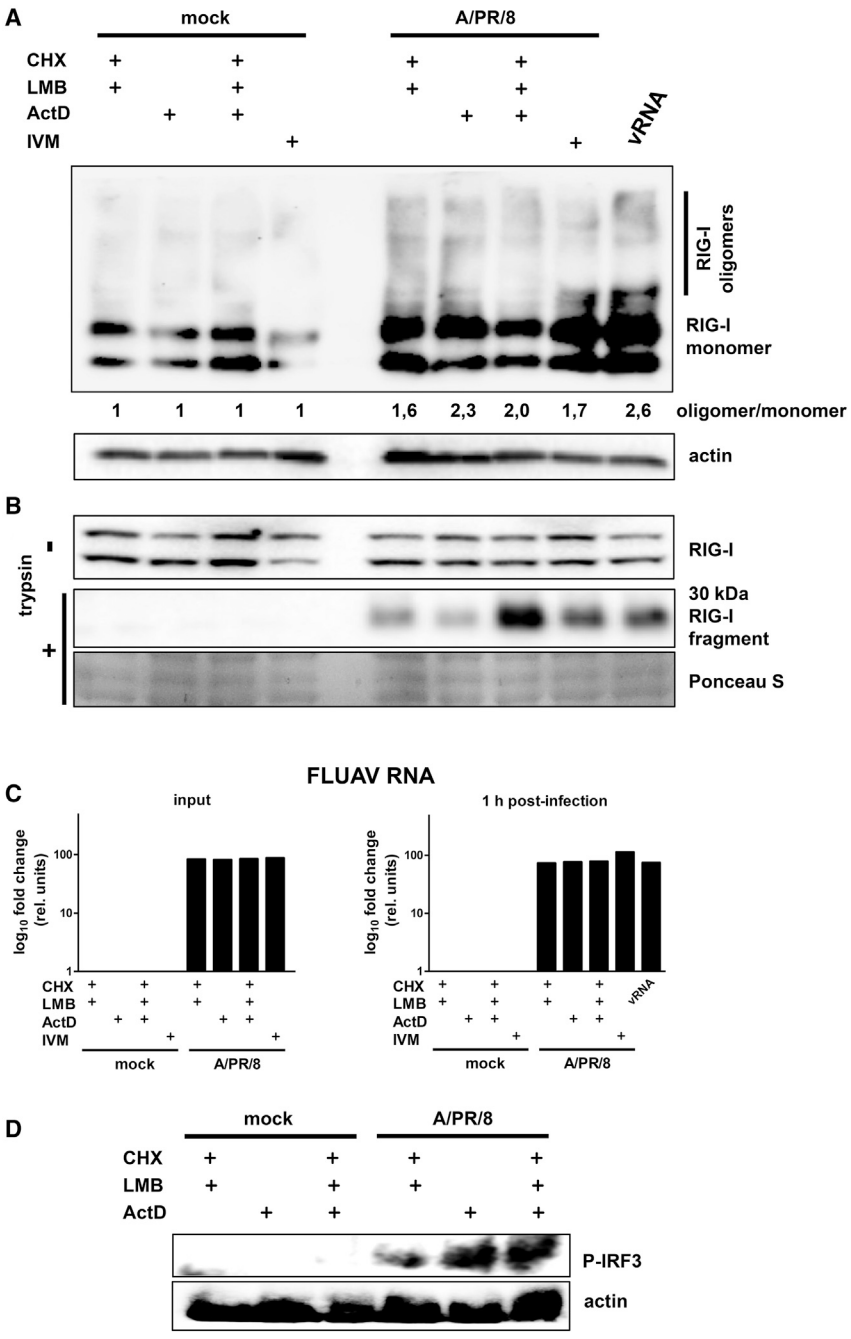

Figure 1. Activation of RIG-I Signaling by Incoming Influenza Virus Nucleocapsids

(A and B) RIG-I activity assays. A549 cells were preincubated for 1 hr with inhibitors, inoculated with strain A/PR/8/34 (moi 1), or left uninfected (mock) for 1 hr at 4°C, incubated 1 hr at 37°C, and analyzed. (A) Oligomerization assay. Lysates of cells treated with CHX (50 μg/ml), LMB (16 nM), ActD (1 μg/ml), or IVM (50 μM) were separated by native PAGE and immunostained for RIG-I. Actin served as loading control. (B) Conformational switch. Lysates as in (A) were subjected to limited trypsin digest and analyzed by RIG-I immunoblot. The Ponceau S protein stain (representative section shown) serves as loading control for the digested samples.

(C) Quantification of total FLUAV segment 7 RNA by RT-qPCR. Input represents RNA amounts harvested after the 1 hr inoculation period at 4°C.

(D) IRF3 activation. A549 cells were pretreated with inhibitors, inoculated with strain A/PR/8/34 (moi 1), or left uninfected (mock) for 1 hr at 4°C, and incubated for 1 hr under inhibitor treatment. Lysates from cells were separated by native PAGE and analyzed by immunoblotting for phosphorylated IRF3 (P-IRF3) and actin as described (Weber et al., 2013). See also Figures S1A–S1C.

RESULTS

Activation of RIG-I by Incoming FLUAV Nucleocapsids

At the onset of infection, the nucleocapsids of FLUAV are released from endosomes to be transported through the cytoplasm and into the nucleus. Only there do they start primary transcription, followed by translation and genome replication. To investigate the interaction between incoming nucleocapsids (and not their RNA products arising later on) and RIG-I in the cytoplasm, we (1) synchronized infection by incubating the virus inoculum at 4°C for 1 hr, (2) allowed the subsequent infection at 37°C to proceed for only 1 hr, and (3) added various inhibitors to ensure restriction to the immediate early infection phase. The inhibitors were cycloheximide (CHX; blocks protein synthesis and therefore viral genome replication), leptomycin B (LMB; inhibits nuclear export of nucleocapsids), and actinomycin D (ActD; inhibits viral transcription) (see Figure S1A available online). In addition, we tested ivermectin (IVM), which is known to block the nuclear import machinery (Wagstaff et al., 2012). Human A549 cells were pretreated with one or several of the inhibitors and 1 hr infected with strain A/PR8/34 (H1N1) at a multiplicity of infection (moi) of 1 as outlined above. Irrespective of the inhibitor, incoming FLUAV nucleocapsids triggered two markers of RIG-I activation: the formation of homo-oligomers (Figure 1A), and the conformational switch reflected by a partial

panhandles also in the physiological context, when packaged by viral NP and polymerase into nucleocapsids (Weber et al., 2013). That study, however, had focused on the cytoplasmically replicating bunyaviruses. Therefore, it remained open whether the panhandles of FLUAV nucleocapsids could also be sensed by the cytoplasmic RIG-I, and whether this occurs during the passage of the incoming nucleocapsids from the endosome to the nucleus early in infection. Here, we report that the transiting FLUAV nucleocapsids are indeed recognized and directly impaired by RIG-I, and that the degree of RIG-I sensitivity varies depending on adaptive mutations in the polymerase subunit PB2.

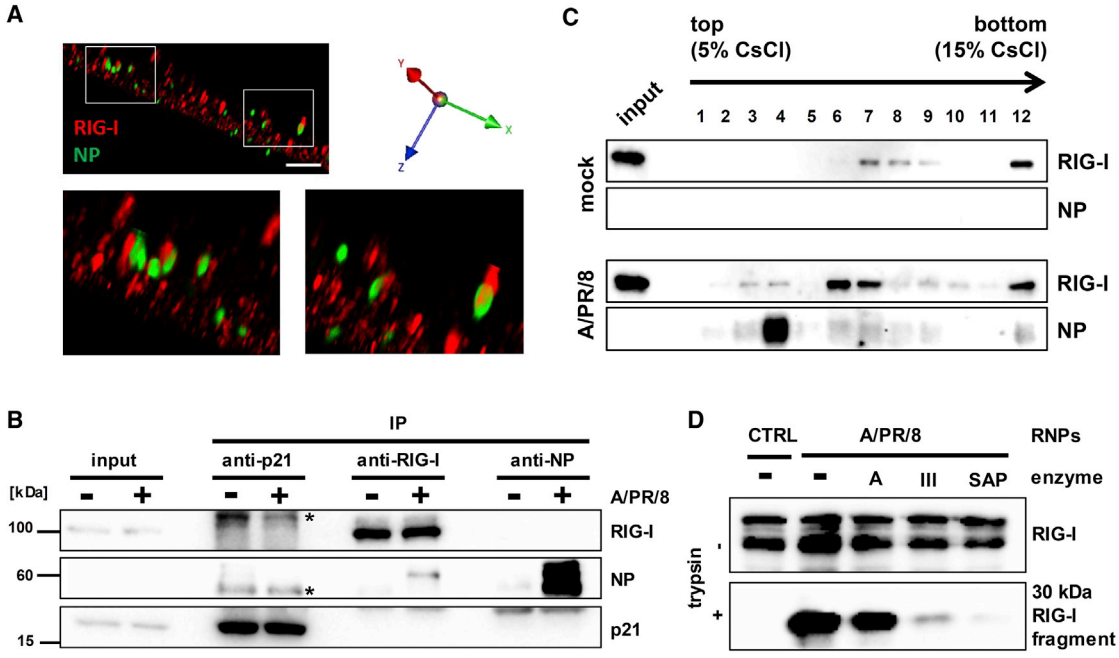

Figure 2. RIG-I Interacts with Incoming Influenza Virus Nucleocapsids and Is Activated in a 5′ppp-dsRNA-Dependent Manner

(A–C) CHX / LMB-treated A549 cells were infected with A/PR/8/34 (moi 1) for 1 hr. (A) Cells analyzed for RIG-I and FLUAV by 3D GSD superresolution immunofluorescence microscopy. Scale bar, 1 μm. Insets are digitally magnified and shown below the main image (taken from one individual cell). (B) Coimmunoprecipitation. Cell lysates were subjected to immunoprecipitation (IP) using antibodies against p21 (negative control), RIG-I, or FLUAV NP and analyzed by immunoblot. Input control is 2% of the lysate. Asterisks (*) indicate unspecific bands. (C) Cosedimentation assay. Cell lysates were separated by a discontinuous CsCl gradient (2% lysate as input control) and fractions analyzed by immunoblotting.

(D) Conditions for activation of RIG-I by nucleocapsids in vitro. Dialyzed lysate of RIG-I-expressing S2 cells was mixed with nucleocapsids of strain A/PR/8/34 (RNPs) or a control preparation (CTRL) and supplemented with 1 mM ATP. The nucleocapsids had either been pretreated with 5 μg RNase A (A), 1 U RNase III (III), or 2 U shrimp alkaline phosphatase (SAP) or left untreated (–) for 1 hr at 37°C. RIG-I conformational switch was assayed after 1 hr of nucleocapsid coincubation at 37°C. See also Figures S2A–S2K.

trypsin resistance (Figure 1B). RIG-I activation by incoming nucleocapsids was comparable to levels obtained by 1 hr transfection of naked virus particle RNA (vRNA). Quantification by RT-qPCR demonstrated the expected absence of viral RNA synthesis (Figures 1C and S1B). In line with this, transcription inhibition by various NTP-depleting agents also had no influence on RIG-I activation by FLUAV (Figure S1C). Nonetheless, not only RIG-I but also its downstream target IRF3 was activated by the incoming nucleocapsids (Figure 1D). It must be remarked that in all our experiments, virus stocks were used which were free of defective interfering particles (data not shown), a known activator of RIG-I (Baum et al., 2010). Moreover, in agreement with a previous study (Killip et al., 2014), we noted that addition of ActD to the mix containing CHX and LMB results in occasional background activation of antiviral signaling in uninfected cells (data not shown). We therefore conducted the majority of subsequent experiments with CHX/LMB treatment and within the short, 1 hr period of synchronized infection, conditions that were optimal for robustly studying interactions of RIG-I with incoming nucleocapsids.

RIG-I Binds to the Panhandle on FLUAV Nucleocapsids

Confocal microscopy revealed that the incoming nucleocapsids are colocalizing with RIG-I, but not with the related helicase MDA5 (Figure S2A; data not shown). Superresolution microscopy suggests that RIG-I directly attaches on one side of the rod-like nucleocapsids (Figure 2A). The stability of these cocomplexes was tested by pull-down experiments. Although the viral input was barely detectable, as expected for a 1 hr infection, the RIG-I immunoprecipitates contained enriched amounts of NP (Figure 2B), indicating interaction of RIG-I with incoming nucleocapsids. Again, this was not dependent on viral RNA synthesis (Figure S2B). When cell lysates were separated in a CsCl gradient, we observed a partial, virus-induced shift of RIG-I from higher-density fractions toward the lower-density fractions which also contained the nucleocapsids (Figure 2C; fractions 7, 8, and 9 in uninfected cells versus fractions 3, 4, and 6 in infected cells). RIG-I was also activated and shifted toward lower-density CsCl fractions when its ATPase activity was inhibited with ADP●AlF_3, suggesting that complex formation is independent of downstream events (Figures S2C–S2E). We also used our insect cell/in vitro system (Weber et al., 2013). Extracts of *Drosophila* S2 cells expressing human RIG-I were dialyzed and supplemented with ATP (to support RIG-I activation). The recombinant RIG-I reacted to purified and dialyzed FLUAV nucleocapsids by conformational switching, oligomerization, and a shift of RIG-I fractions in the CsCl gradient (Figures S2F–S2H). To test the structural determinants of RIG-I activation, purified FLUAV nucleocapsids were pretreated in vitro with enzymes. Both destruction of dsRNA by RNase III and cleavage of the

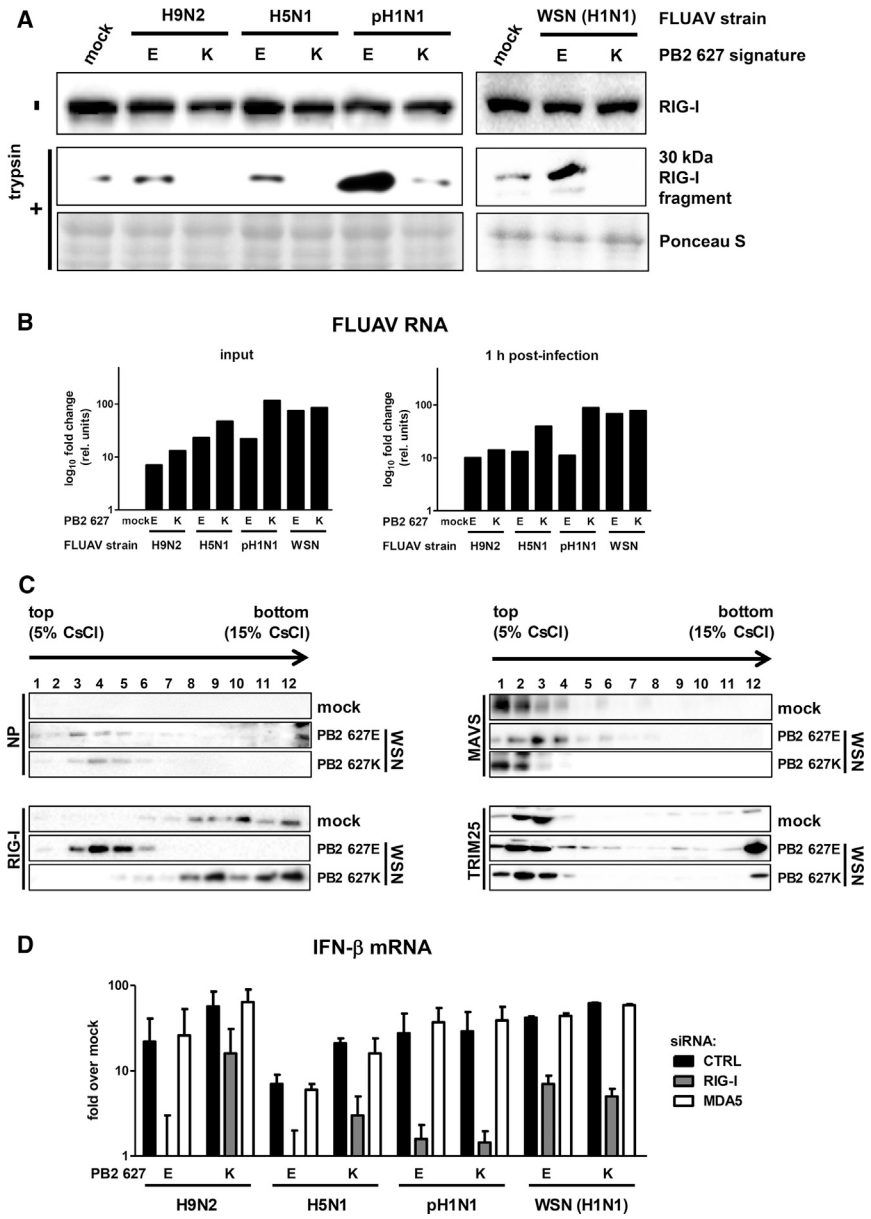

Figure 3. Adaptive Mutations in PB2 Influence the Activation of RIG-I by FLUAV Nucleocapsids

(A) RIG-I activation by viruses with different PB2-627 signatures. Cells were infected with strains of A/quail/Shantou/2061/00 (H9N2), A/Thai/KAN-1/04 (H5N1), A/Hamburg/05/2009 (pH1N1), or A/WSN/33 (H1N1) containing avian-signature E or mammalian-signature K at PB2-627. Infections, CHX/LMB treatment, and RIG-I conformational switch testing were performed as described for Figures 1 and 2.

(B) Quantification of virus RNAs by RT-qPCR for genomic segment 7. Input represents RNA amounts harvested after the 1 hr infection period.

(C) Cosedimentation assay. Lysates of cells infected with PB2 variants of A/WSN/33 (H1N1) using our standard 1 hr protocol were separated by a CsCl gradient and analyzed by immunoblotting.

(D) RIG-I-dependent IFN induction by incoming nucleocapsids. A549 cells were transfected with the indicated siRNAs or a negative control siRNA (CTRL). A549 cells siRNA depleted of RIG-I or MDA5 were pretreated with CHX and LMB, and infected with FLUAV strains (moi 1) for 16 hr. IFN-β mRNA levels were determined by real-time RT-PCR. Mean and SDs from three independent experiments are shown. See also Figures S3A–S3H.

5′ppp by a phosphatase aborted RIG-I stimulation, whereas the ssRNA-specific RNase A had no such effect (Figure 2D). Importantly, RIG-I activation did not depend on the specific nucleocapsid preparation method, and was also observed for nucleocapsids that were affinity purified via a strep-tagged PB2 subunit (Figures S2I–S2K). Also, cotransfection experiments demonstrated that the pull-down of NP by RIG-I is dependent on the genomic RNA, and not on protein-protein interactions (see below). Together, these data suggest that RIG-I directly interacts with the 5′ppp dsRNA panhandle on intact FLUAV nucleocapsids and in a manner that is independent of mammalian cofactors or viral RNA synthesis.

PB2 Is a RIG-I Antagonist

Avian FLUAV strains need to acquire adaptive mutations to establish infection in mammals. A major determinant of host switching and virulence is the polymerase subunit PB2 (Hatta et al., 2001). PB2 position 627, in particular, carries in avian strains a glutamic acid (E), but in most mammalian-adapted strains a lysine (K) (Subbarao et al., 1993). The reason for the mammalian selection pressure toward PB2-627K is not fully understood (Cauldwell et al., 2014; Mänz et al., 2013). Interestingly, however, chickens are known to be deficient in RIG-I (Barber et al., 2010). Using the conformational switch assay, we investigated whether RIG-I might be involved in the mammalian-specific effects on avian-signature PB2 polymerases. Human A549 cells were exposed to the immediate early infection phase of variants of four FLUAV strains, A/quail/Shantou/2061/00 (H9N2), A/Thai/KAN-1/04 (H5N1), pandemic A/Hamburg/05/2009 (pH1N1), or A/WSN/33 (H1N1). In all cases, those viruses with the avian signature PB2-627E activated RIG-I much more strongly than those with the mammalian signature PB2-627K (Figures 3A and S3A). These differences were not due to variations in input RNA or RNA synthesis, as viral RNA levels were comparable and did not increase during the 1 hr experiment (Figures 3B and S3B–S3D). Also in CsCl gradient assays, we observed a more pronounced shift of RIG-I fractions in response to a PB2-627E virus (Figure 3C, left panels). The PB2-627E virus also relocalized the RIG-I interactors MAVS and TRIM25 (Figure 3C, right panels), further supporting the notion of a stronger RIG-I activation by the avian-signature nucleocapsids.

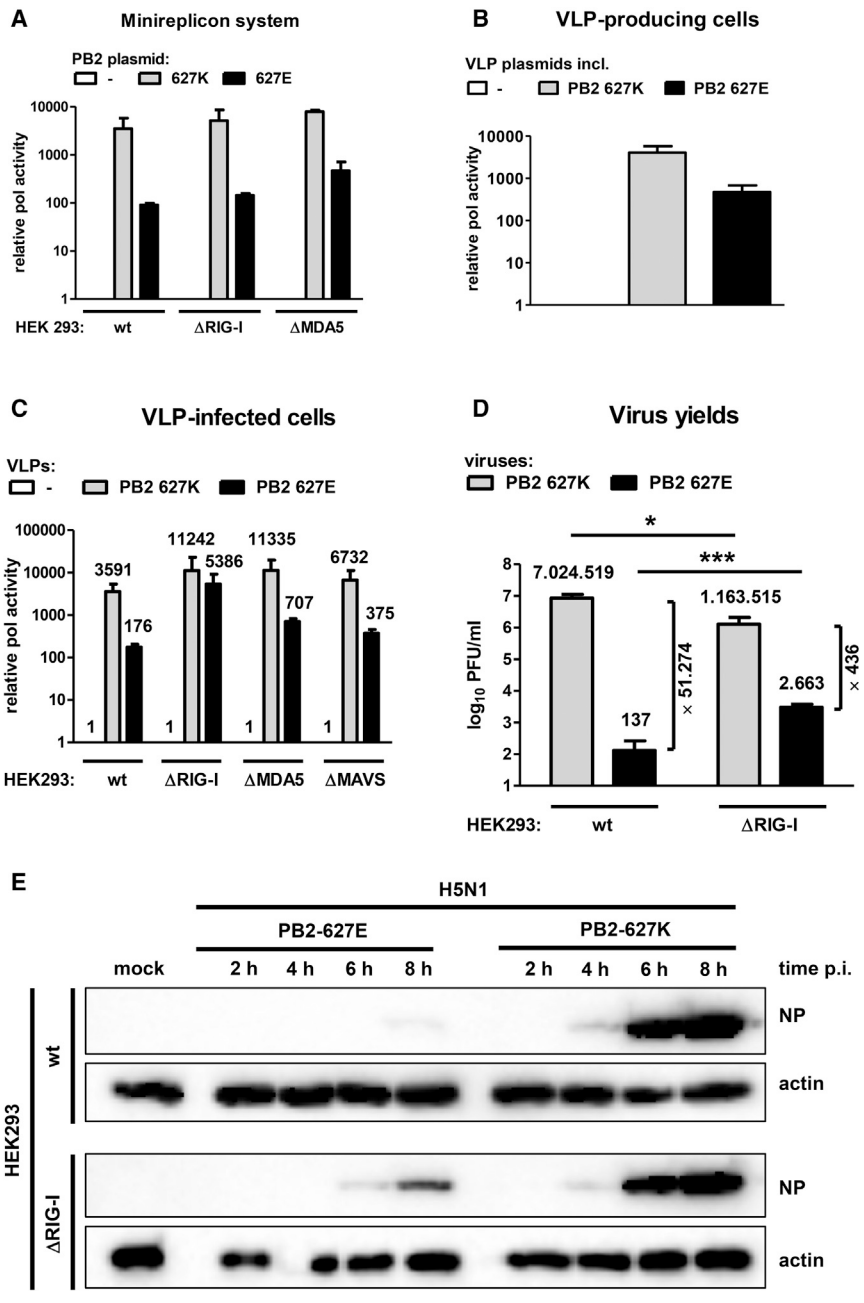

Figure 4. RIG-I Evasion by PB2-E627K

(A) Activity of A/WSN/33-based minireplicon systems containing PB2-627K, -627E, or no PB2 (–) in HEK293 WT, *ΔRIG-I*, or *ΔMDA5* cells.

(B) Reporter activities in HEK293 cells producing VLPs containing nucleocapsids with the indicated PB2 signatures.

(C) Reporter activities in WT and deletion cells infected with VLPs. Cells had been pretransfected with PB1, PA, NP, and matching PB2.

(D) Multicycle virus kinetics. 293 WT or *ΔRIG-I* cells were infected with the indicated PB2 variants of strain A/Thai/KAN-1/04 (H5N1) at an moi of 0.0001. Virus yields were determined 24 hr later by plaque assay. In all cases, mean and SDs from three independent experiments are shown.

(E) Single-cycle virus kinetics. Cells were infected at an moi of 1 and monitored for NP expression over time. See also Figures S4A–S4D.

The A/PR/8/34 strain used for the initial RIG-I activation experiments (see Figures 1 and 2) contains PB2-627K (Foeglein et al., 2011). A comparison of A/PR/8/34 with PB2-627K and –627E variants of A/WSN/33 (H1N1) demonstrates its relatively weak RIG-I activation potential (Figure S3E), thus being in line with the correlation between reduced RIG-I activation and the PB2-627K signature. Virus-like particles containing a A/WSN/33 (H1N1) reporter minigenome (VLPs) showed the same PB2-627-dependent phenotype, independent of the particular envelope protein (Figure S3F). This confirms that nucleocapsids are the critical component. As expected, RIG-I activation by PB2-627E virus was independent of any viral RNA synthesis (Figure S3G). We also measured IFN induction obtained after overnight infection by the different FLUAV strains, again under CHX and LMB. Surprisingly, despite the clear effects on RIG-I activation described above, there were no consistent PB2-627-dependent differences in IFN induction, both in WT and in RIG-I- depleted knockdown cells (Figures 3D and S3H). Of note, human-adapted PB2-627K has a higher polymerase activity in mammalian cells (Naffakh et al., 2000) but nonetheless activated RIG-I much more weakly than PB2-627E. This again argues against RNA synthesis as a trigger of RIG-I. Collectively, our data indicate that the adaptive mutation PB2-E627K represents a viral countermechanism to RIG-I recognition, even if it has no significant effect on IFN induction.

RIG-I Influences Infection by Incoming PB2-627E Nucleocapsids

PB2-627E confers reduced polymerase activity in mammalian cells, whereas in avian cells the activity is similar to PB2-627K (Massin et al., 2001; Paterson et al., 2014). The species-specific differences were attributed to a mammalian restriction factor acting on PB2-627E only (Mehle and Doudna, 2008). We wondered whether RIG-I could be contributing to PB2-627E suppression in mammalian cells. The classic assay for measuring FLUAV polymerase activity is the minireplicon reporter system, consisting of plasmid-expressed polymerase subunits and NP that encapsidate, transcribe, and replicate a reporter minigenome bearing panhandle sequences. Minireplicon activity in human 293 WT cells confirmed the difference between the two PB2 variants (Figure 4A). We generated knockout 293 cells (Figure S4A) to test the effect of RIG-I on minireplicon activity but could not detect major differences to WT cells or *MDA5* knockout cells

(see Figure 4A). It needs to be noted, however, that here the recombinant nucleocapsids are not entering the cytoplasm as in infection, but are artificially assembled in the nucleus by the plasmid-encoded proteins. Thus, as an alternative closer to the immediate-early infection situation, we employed VLPs containing recombinant FLUAV nucleocapsids. Reporter activity in the 293 WT cells used to produce VLPs for strain A/WSN/33 (H1N1) differed between the two PB2 variants, as expected (Figures 4B and S4B). However, VLPs with PB2-627E regained considerable activity upon infection of Δ*RIG-I* cells, but not in WT cells or Δ*MDA5* cells (Figure 4C). Curiously, in cells that lacked the RIG-I adaptor MAVS, PB2-627E could also not be rescued, suggesting that signaling may not be necessary (see below). We also tested the influence of RIG-I on viral multiplication. To obtain multicycle growth, we infected 293 WT or Δ*RIG-I* cells for 24 hr with moi 0.0001 of PB2 variants of strain A/Thai/KAN-1/04 (H5N1). The absence of RIG-I rescued the low yields of the PB2-627E virus by one order of magnitude, whereas the PB2-627K virus was slightly reduced (Figure 4D). Overall, the approximately 50,000-fold growth difference between the PB2 signature viruses in WT cells decreased to 400-fold in Δ*RIG-I* cells. Since RIG-I is activated by nucleocapsid entry, we also monitored the initial establishment of infection. WT or Δ*RIG-I* cells were infected with moi 1, and the synthesis of NP was assayed for 8 hr. For PB2-627K viruses, NP was detected from 4 hr p.i. on in both cell types (Figures 4E, S4C, and S4D). For the PB2-627E virus, by contrast, NP was detected at 8 hr p.i. in WT cells, but from 6 hr on in Δ*RIG-I* cells. Since viral entry is affected neither by the PB2 signature nor by the cell genotype (Figure S4E), we conclude that RIG-I targets PB2-627E-type nucleocapsids during the onset of infection.

Species- and Signaling-Independent Antiviral Effect of RIG-I

An unexpected result of our VLP infection experiments (see Figure 4C) was that the attenuated phenotype of incoming PB2-627E nucleocapsids was not rescued by deleting the signaling adaptor *MAVS*. Similarly, also virus with PB2-627E was delayed in Δ*MAVS* cells (Figure 5A). To investigate this further, we transcomplemented Δ*RIG-I* cells with an ATPase-negative RIG-I mutant (K270A) that is unable to signal but still able to bind RNA (Takahasi et al., 2008). Strikingly, the RIG-I K270A mutant was as potent as WT RIG-I in delaying the onset of PB2-627E virus and VLP infection (Figures 5B and S5). This is in line with our observation that chemical ATPase inhibition of RIG-I does not impede activation and nucleocapsid binding (see Figures S2C–S2E). Transcomplementation with human RIG-I also endowed chicken cells with the ability to slow down PB2-627E virus infection (Figure 5C). Again, this was independent of antiviral signaling. These data suggest that the binding of RIG-I to incoming nucleocapsids (see Figures 2 and S2) is sufficient to delay infection by FLUAV strains with the avian PB2-627E signature. Thus, RIG-I signaling may not be required for the restriction of avian strains early in infection.

Nucleocapsid Stability Influences RIG-I Binding and Sensitivity

The 627K adaptation is known to increase the binding of PB2 to NP (Labadie et al., 2007). Although this had been disputed as an artifact of the stronger polymerase activity (and hence nucleocapsid formation) by PB2-627K (Cauldwell et al., 2013), others had shown stronger NP binding by PB2-627K also in a nucleocapsid-free in vitro system (Ng et al., 2012). In our immediate-early infection setup, infection occurred for 1 hr, and the formation of daughter nucleocapsids was impossible due to CHX treatment. Nonetheless, also under these conditions NP coprecipitated more PB2-627K than PB2-627E, confirming the adaptation-specific differences in binding affinity (Figure 6A). Moreover, NP/PB2-627E interactions slightly increased in Δ*RIG-I* cells that were infected (see Figure 6A) or are harboring minireplicon systems (Figures S6A and S6B).

RIG-I directly interacts with the panhandles of FLUAV nucleocapsids (see Figures 2D and S2K). Interestingly, RIG-I pulled down more incoming nucleocapsids of the PB2-627E type than of the PB2-627K type (Figure 6B). Moreover, the PB2 protein of the 627K type was found to be coprecipitated, but not PB2 of the 627E type. Similar results were obtained with recombinant nucleocapids of the minireplicon system, an experimental setup that also allowed us to demonstrate that RIG-I-NP interactions depend on the encapsidated genome RNA (Figure 6C). Thus, nucleocapsids of the PB2-627E type are more efficiently bound by RIG-I.

The lower affinity of PB2-627E to NP may enable RIG-I to better access the nucleocapsid-borne panhandle RNA. This would implicate that the strength of the polymerase-nucleocapsid interaction influences RIG-I activity. To directly test this hypothesis, we disrupted the polymerase complex with a PB1-derived peptide (PB1-T6Y) (Wunderlich et al., 2011). The inhibitor peptide massively increased RIG-I activation by incoming nucleocapsids, and independently of the PB2-627 signature (Figures 6D and S6C). Thus, the strength of polymerase binding, modulated either naturally (by PB2 mutation) or artificially (by disrupting PB1-PA interactions), sensitizes nucleocapsids to RIG-I.

In summary, our results indicate that FLUAV nucleocapsids are prone to signaling-independent RIG-I inhibition during their passage through the cytoplasm early in infection. RIG-I recognizes the panhandle structure on the viral genome RNA, which is normally bound by the polymerase complex. The sensitivity to RIG-I is determined by the well-known host adaptation at PB2-627, which affects the binding affinity of PB2 to nucleocapsids. Thus, RIG-I apparently represents one of the mammalian restriction factors driving adaption of avian FLUAV strains toward tighter polymerase binding.

DISCUSSION

An outstanding feature of influenza viruses is the replication in the nucleus. This allows access to the cellular transcription and splicing machineries, and—as our results suggest—the hiding from cytoplasmic RIG-I during most phases of the infection cycle. In fact, since orthomyxoviruses are also unique with respect to the unusually high number of genome segments (and hence RIG-I ligands), it is possible that moving into the nucleus initially evolved as a RIG-I counterstrategy. In line with this, efficient interaction with the nuclear import machinery was shown to be a determinant of host adaptation (Gabriel et al., 2011; Hudjetz and Gabriel, 2012; Resa-Infante et al., 2008). However, the virus

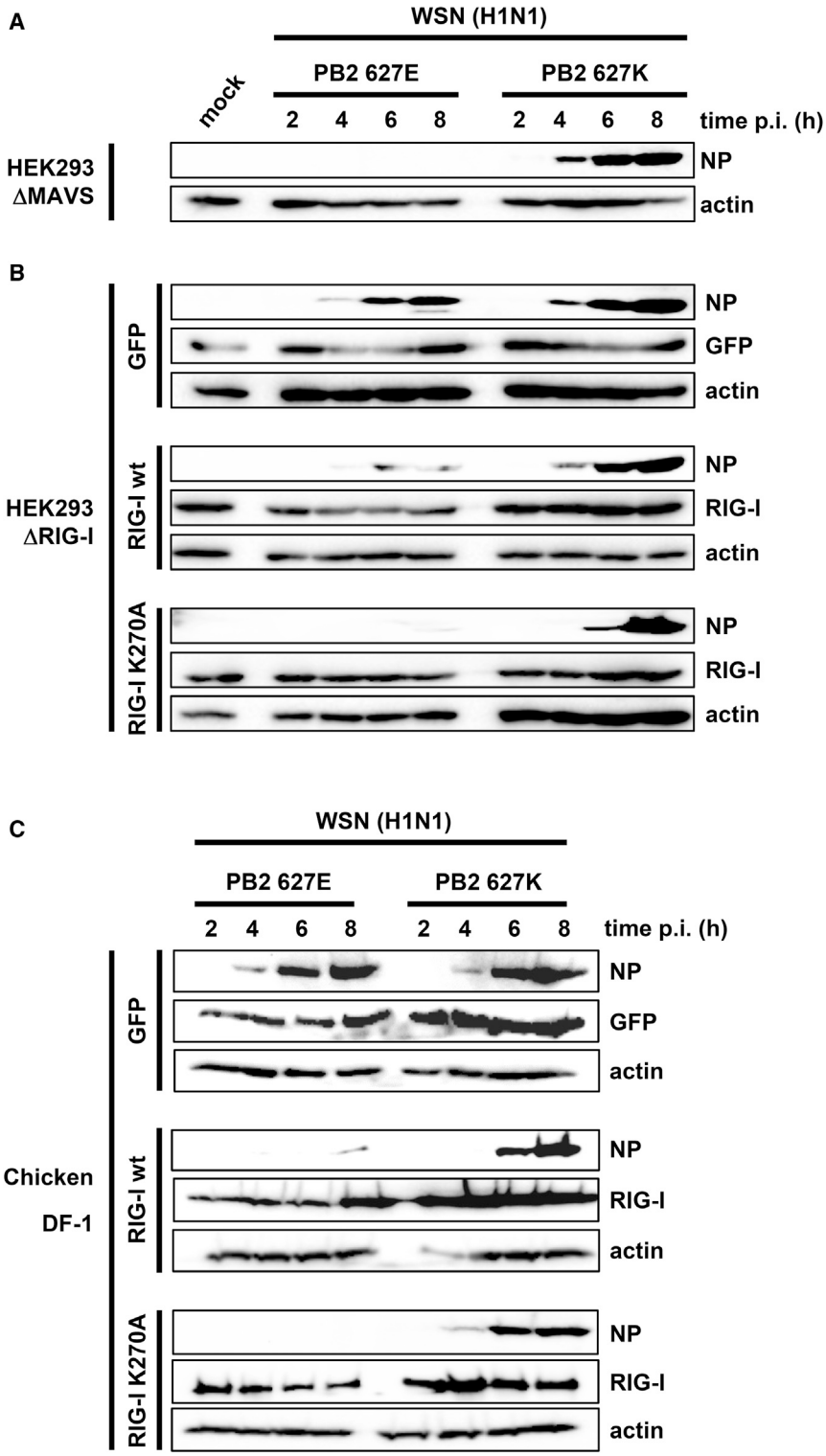

Figure 5. Signaling-Independent RIG-I Effect on Early Infection

Single-cycle infection kinetics of A/WSN/33 on human cells lacking MAVS (A) or RIG-I (B), or on chicken DF-1 cells that naturally lack RIG-I (C). The *ΔRIG-I* and the DF-1 cells were transiently transfected with plasmids encoding GFP (negative control), FLAG-RIG-I WT, or FLAG-RIG-I K270A, as indicated. Overexpression was controlled using antibodies against GFP or the N-terminal Flag tag of the RIG-I constructs. See also Figure S5.

remains vulnerable during the transit to the nucleus, since at this stage of infection neither the classic IFN antagonist NS1 (Hale, 2014) nor the host response suppressors PA-X (Jagger et al., 2012) or PB1-F2 (Varga et al., 2011) would be expressed. Therefore, it appears plausible that the nucleocapsids themselves have to cope with the pathogen recognition system, an assumption that is in agreement with our data and also with previous reports that FLUAV polymerase subunits can prevent IFN induction (Marcus et al., 2005; Pérez-Cidoncha et al., 2014) and interact with RIG-I and MAVS (Graef et al., 2010; Iwai et al., 2010; Li et al., 2014; Liedmann et al., 2014). Moreover, for influenza B virus it was demonstrated that nucleocapsids were sufficient to induce IFN, whereas for FLUAV RNA synthesis was required (Österlund et al., 2012). These comparative data again point toward nucleocapsids being able to both induce and suppress innate immunity, dependent on the genetic background.

The connection between RIG-I activation and IFN induction is not straightforward. Avian FLUAV strains that strongly activated RIG-I were in fact IFN inducers weaker than or equal to the mammalian strains whose nucleocapsids had inhibited RIG-I. Most likely, the underlying reason is found in the differences in RNA polymerase activities, which are inseparable from the RIG-I inhibition capacity. While PB2-627E nucleocapsids have low RNA synthesis rates but are strong activators of RIG-I, PB2-627K nucleocapsids have a highly active polymerase but inhibit RIG-I. Thus, the RIG-I inhibition by PB2-627K might be overwhelmed by the higher RNA synthesis rate.

It was previously stated that IFN induction by FLUAV occurs exclusively through RNA synthesis products (Killip et al., 2014; Österlund et al., 2012). However, we observed IRF3 activation by incoming nucleocapsids even when viral transcription was shut off by ActD treatment. This appears to contradict the results by Killip et al., who had not seen any such IRF3 activation (Killip et al., 2014). However, in that study IRF3 was assayed at 8 hr postinfection, a time point at which IRF3 activity may have waned, as IRF3 returns to the inactive state in case of

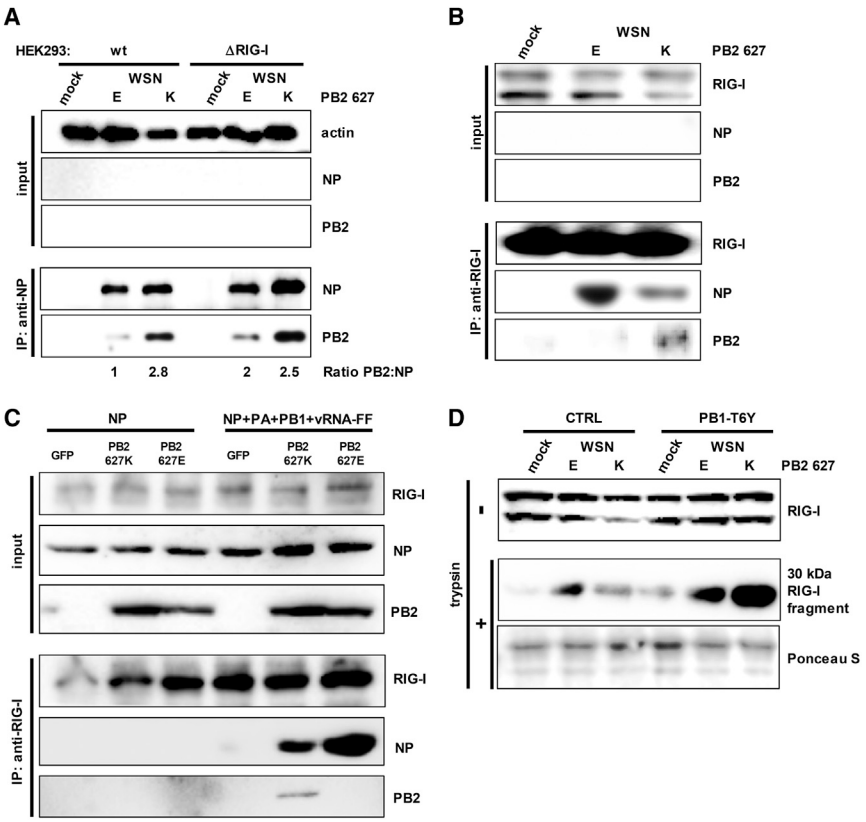

Figure 6. Effect of the PB2 627 Signature on Protein-Protein Interactions

(A) NP immunoprecipitation. Cells were CHX/LMB treated and infected with A/WSN/33 strains carrying PB2-627K or 627E as described for 1A. Lysates were immunoprecipitated 1 hr later with anti-NP and immunoblotted as indicated. Normalized quantifications of the immunoprecipitated proteins are shown below. Note that amounts of viral input proteins are too low to be detected in the total extracts.

(B) RIG-I immunoprecipitations from infected cells. HEK293 cells were infected with A/WSN/33 PB2 variants as described for Figure 1A. Immunoprecipations with anti-RIG-I and immunoblotting were performed as indicated for Figure 2B.

(C) RIG-I immunoprecipitations of recombinant nucleocapsids. HEK293 cells were transfected with A/WSN/33 NP combined with GFP or the PB2 variants (left panel), or with all A/WSN/33 minireplicon plasmids (right panel). Immunoprecipations with anti-RIG-I were performed as indicated in (B).

(D) Polymerase destabilization. A549 cells were infected with PB2 variants of strain A/WSN/33 (moi 1), treated with peptides Borna-X-Tat (CTRL) or $PB1_{1-15}$ T6Y-Tat (PB1-T6Y), and tested for RIG-I conformational switch 1 hr postinfection. See also Figures S6A–S6C.

low inducers (Long et al., 2014). We therefore propose that incoming FLUAV nucleocapsids can activate RIG-I and antiviral signaling, similar to those of influenza B virus (Österlund et al., 2012) and the cytoplasmic RNA viruses (Weber et al., 2013). IFN induction by nucleocapsids is, however, comparatively weak, and the subsequent RNA synthesis becomes the dominant IFN elicitor once the nucleocapsids have reached the nucleus.

Although PB2-627K had no apparent bearing on IFN induction, for PB2-627E viruses and VLPs the establishment of infection was slowed down by RIG-I. Strikingly, while deletion of *RIG-I* accelerated infection by avian strains, deletion of the downstream adaptor *MAVS* did not. Moreover, a signaling-inactive mutant of RIG-I was as potent as WT RIG-I itself in slowing down PB2-627E viruses. It is therefore likely that the binding of RIG-I to the panhandle RNA results in a direct (although transient) antiviral effect against avian strains. The mammalian-adapted nucleocapsids are more efficient in hiding their panhandle, and it could be speculated that this is due to the stronger binding of the PB2 to the NP. The signaling-independent antiviral effect may also explain why RIG-I follows the nucleocapsids into the nucleus at the late stage of infection (Li et al., 2014).

Besides PB2-627K, there might be more factors influencing the RIG-I sensitivity of nucleocapsids. The circulating 2009 pandemic pH1N1 strains have retained the PB2-627E signature but acquired compensating second-site mutations (Mehle and Doudna, 2009; Yamada et al., 2010). Nonetheless, our direct comparisons between variants of four FLUAV strains that differed only in position PB2-627 strongly indicate that this major adaptation is in fact a RIG-I escape mechanism. It will be interesting to see whether other adaptive mutations in the polymerase or the NP also affect RIG-I.

FLUAV epidemics feed from avian reservoirs. Wild bird species, e.g., ducks, express functional *RIG-I*, but domestic chicken do not (Barber et al., 2010; Kowalinski et al., 2011). Many avian FLUAV strains cause asymptomatic infection, e.g., in ducks, but an acute systemic disease in chicken (Kim et al., 2009). Populations of wild birds are comparatively disperse, i.e., overt disease would reduce the chance of viral spread. Chickens, by contrast, are held under crowded conditions and with a constant, nonnatural replenishment of susceptible individuals. A certain RIG-I sensitivity may allow FLUAV to persist in the wild bird reservoir. In domestic chickens, there is no selection pressure on sparing the host, and the absence of RIG-I could enable rapid viral spread. In humans, the viral transmission mode requires replication to levels causing respiratory symptoms. Hence, it could be speculated that mutations suppressing RIG-I activation are needed for efficient and sustainable infection of humans, but not in chicken (no RIG-I) or wild birds (RIG-I enables asymptomatic infection). While RIG-I appears to be acting on incoming nucleocapsids of avian-adapted viruses, other host cell factors are likely to contribute to the PB2-directed host restriction during later stages of infection.

Applying a polymerase-disrupting peptide massively increased RIG-I activation by nucleocapsids. This uncovers the full potential of RIG-I and implies that even for avian-adapted strains only a fraction of the nucleocapsids is actually

recognized. Therefore, drugs targeting the FLUAV polymerase complex will have the secondary benefit of boosting antiviral host responses.

In sum, our data indicate that incoming FLUAV nucleocapsids are prone to a direct antiviral inhibition by RIG-I, and that the degree of RIG-I sensitivity is dependent on nucleocapsid stability.

EXPERIMENTAL PROCEDURES

Cells and Viruses

A549, HEK293, DF-1, MDCK II, and *Drosophila* S2 cells were cultivated as described (Weber et al., 2013). FLUAV A/PR/8/34, the recombinant strains of A/quail/Shantou/2061/2000 (H9N2) (Baron et al., 2013), A/Hamburg/05/2009 (pH1N1), A/WSN/33 (H1N1), and A/WSN/33 with Strep-tagged PB2 (Rameix-Welti et al., 2009) were grown on MDCK II cells. A/Thai/KAN-1/04 (H5N1) was grown on chicken DF-1 cells (Manz et al., 2012). All viruses were entirely sequenced and confirmed to harbor only the intended mutations.

Infections

Cells were washed once with phosphate-buffered saline (PBS) and inoculated for 1 hr at 4°C with virus dissolved in OptiMEM (Invitrogen) or 250 μl cell supernatant containing VLPs. The inoculum was replaced with DMEM containing 0.2% BSA and (except for VSV-G VLP infections) 1 μg/ml L-1-tosylamido-2-phenylethyl chloromethyl ketone (TPCK)-treated trypsin (Sigma-Aldrich), and cells were further incubated at 37°C.

RIG-I Activation Assays

Analyses of RIG-I conformation and oligomerization were described elsewhere (Weber et al., 2013; Weber and Weber, 2014a). For cosedimentation assays from mammalian cells, cell lysates were prepared as for coimmunoprecipitation (see below). The cleared lysates were loaded on a discontinuous 5%–15% CsCl gradient in 20 mM Tris/HCl (pH 7.9), 200 mM NaCl, and centrifuged at 52,000 rpm for 2 hr at 12°C in a SW60 rotor (Beckman). Altogether 12 fractions were recovered from top to bottom and pelleted at 45,000 rpm for 1 hr at 4°C in a TLA45 rotor (Beckman). Pellets were dissolved in sample buffer, boiled for 5 min, and analyzed by immunoblotting. Proteins were detected with rabbit polyclonal anti-A/quail/Shantou/2061/00 (H9N2) (Baron et al., 2013) at 1:8,000 and the mouse monoclonals anti-RIG-I ALME-1 (Enzo Life Sciences; 1:1,000), anti-MAVS (Abcam; 1:500), and anti-human TRIM25 (BD Transduction Laboratories, 1:5,000).

Cosedimentation assays with S2 cell samples were performed by a similar procedure. Briefly, 50 μl dialyzed lysates (containing 100 μg protein) were mixed with 50 μl of dialyzed PR/8/34 nucleocapsids and supplemented with 1 mM ATP. After 1 hr at 37°C the samples were analyzed using a discontinuous 10%–30% CsCl gradient.

Inhibitor Treatments

CHX, $CuSO_4$, ActD, and IVM were purchased from Sigma Aldrich and LMB from Biomol. Cells were pretreated with CHX (50 μg/ml, stocks dissolved in DMSO), LMB (16 nM, stocks dissolved in ethanol), ActD (1μg/ml, stocks dissolved in DMSO), or IVM (50 μM, stocks dissolved in DMSO) for 1 hr before infection. Inhibitors were also included in the virus inoculum, and the incubation medium. ADP●AlF_3 treatment was performed as described (Weber et al., 2013).

Immunofluorescence Microscopy

For superresolution immunfluorescence by ground state depletion (GSD) microscopy, samples were prepared as described for confocal microscopy (see Supplemental Information) with minor modifications. As secondary antibodies, donkey anti-rabbit Alexa Fluor 555 (FLUAV) and goat anti-mouse Alexa Fluor 647 (RIG-I) were used, and samples were embedded in 50 mM Tris-HCl (pH 8.0) dissolved in 10% Vectashield mounting medium (VectorLabs) and 90% glycerol. Analysis was performed with the Leica SR GSD microscope.

Purification of Native Viral Nucleocapsids

MDCK II cells were seeded in nine T175 cell culture flasks at a confluency of 40% and infected with FLUAV strain PR/8/34 at an moi of 0.01 or left uninfected (control). Supernatants were harvested at 48 hr p.i., and nucleocapsids were purified as described (Weber et al., 2013).

Coimmunoprecipitation Assay

Immunoprecipitations using mouse monoclonals anti-p21 (Santa Cruz Biotechnology) and anti-RIG-I (ALME-1) were performed as described (Weber et al., 2013). Mouse monoclonal anti-NP (HB65) (Wisskirchen et al., 2011) was used at a 1:200 dilution in RIPA buffer. Mouse monoclonals anti-p21 (1:500), anti-RIG-I ALME-1 (1:1,000), and rabbit polyclonal H9N2 (1:8,000) were used for immunoblotting.

Enzymatic Treatment of Nucleocapsids

Dialyzed nucleocapsids were treated with RNase A, RNase III, or SAP and incubated with dialyzed lysates from RIG-I-expressing S2 cells (supplemented with 1 mM ATP) as described (Weber et al., 2013).

Real-Time RT-PCR

RNA was isolated from cells using the RNeasy Mini Kit (QIAGEN), and 10 ng was analyzed with the one-step QuantiTect SYBR Green RT PCR kit (QIAGEN) in a StepOne Real-Time-PCR-Cycler (Applied Biosystems). Cellular RNA was quantified with specific QuantiTect primers against IFN-β (QT00203763) and γ-actin (QT00996415). For detection of FLUAV segment 7 sequences, reverse transcription was performed using the QIAGEN QuantiTect Reverse Transcription Kit with the (−) strand-specific forward (5′-GGACTGCAGCGTAGACGCTT-3′) and (+) strand-specific reverse primer (5′-CATCCTGTTGTATATGAGGCCCAT-3′). PCR was performed using QuantiTect SYBR Green PCR. Values were normalized against γ-actin using the ΔΔCT method (Livak and Schmittgen, 2001). Upregulation of inducible genes is depicted in relation to nonstimulated, noninfected (mock) cells.

siRNA Knockdown

A549 cells were twice reverse transfected with predesigned siRNAs from QIAGEN (AllStar Negative Control siRNA and FlexiTube siRNAs against RIG-I [SI03649037] and MDA5 mRNA [GS23586]). For each siRNA, 25 nM was diluted in 100 μl DMEM, supplemented with 1 μl Lipofectamine RNAiMAX Reagent (Invitrogen), and incubated for 15 min at room temperature. The siRNA transfection mixes were transferred into a 24-well plate, and 1 × 10E5 cells dissolved in 900 μl DMEM 10% FCS were seeded on top. After 48 hr of incubation at 37°C with 5% CO_2, cells were harvested, and 1 × 10E5 cells were again reverse transfected as described above and incubated for additional 24 hr at 37°C with 5% CO_2.

Generation of Knockout Cell Lines

Using GeneJuice reagent (Merck), 2.5 × 10E4 HEK293T cells were transfected with plasmids for either a zinc finger nuclease targeting the *RIG-I* gene or for a pair of transcription activator-like effectors to nucleases targeting the genes for *MDA5* or *MAVS*. Two days later, 0.5 cells per well were seeded into six 96-well plates. After 2 weeks, colonies were trypsinized and seeded into two replica plates. The next day, one of the replicates was lysed (0.2 mg/ml Proteinase K, 1 mM $CaCl_2$, 3 mM $MgCl_2$, 1 mM EDTA, 1% Triton X-100, 10 mM Tris [pH 7.5]). Genotypes were obtained by sequencing PCR amplicons covering the target site of interest (target sequences and primer sequences available upon request). For each target gene, a clone was selected that had all alleles disrupted.

VLP System

HEK293 cells were transiently transfected with plasmids in 2 μl GeneJammer (Agilent) per 1 μg DNA, and medium was changed after 4 hr. VLPs for strain A/WSN/33 were generated as described (Neumann et al., 2000). HEK293 WT cells were transfected with plasmids for VSV-G oder FLUAV HA (1 μg), as well as M1 (2 μg), M2 (100 ng), NEP (1 μg), PB2-627E or PB2-627K (1 μg), PB1 (1 μg), PA (100 ng), NP (1 μg), a firefly luciferase minigenome construct (1 μg), and a Renilla luciferase construct (pRL-SV40; 75 ng). As negative control, PB2 was replaced by additional PB1 plasmid. Two days later supernatants were collected and treated with 25 U/ml Benzonase (Novagen) for 3 hr

at 37°C. Cleared cell supernatants were used for VLP infections of HEK293 cells (pretransfected with NP, PA, PB1, and the matching PB2) as described above. Luciferase activities were measured 48 hr posttransfection (VLP-producing cells) or infection (VLP-infected cells). Firefly luciferase activity was normalized against Renilla activity. Relative polymerase activity is depicted as fold induction with respect to mock control.

Peptide Inhibitor Treatment

A549 cells seeded at 80% confluency in T25 flasks were washed once with PBS and infected with A/Thai/KAN-1/04 (moi 1) for 1 hr at 4°C. Then, cells were treated with 10 ng/ml Borna-X-Tat or $PB1_{1-15}$ T6Y-Tat (Wunderlich et al., 2011) dissolved in medium with 0.2% BSA. At 1 hr posttreatment, cells were lysed and subjected to the RIG-I conformational switch assay.

SUPPLEMENTAL INFORMATION

Supplemental Information includes six figures and Supplemental Experimental Procedures and can be found with this article at http://dx.doi.org/10.1016/j.chom.2015.01.005.

ACKNOWLEDGMENTS

We thank Silke Stertz and Jovan Pavlovic for the kind gift of anti-PB2 and anti-NP antibodies. We are indebted to the Drug Synthesis and Chemistry Branch of the National Cancer Institute for donating NTP-depleting agents. Work in the F.W. laboratory is supported by the DFG grants We 2616/7-1 of SPP 1596, SFB 593 and SFB 1021, by the Forschungsförderung gem. §2 Abs. 3 Kooperationsvertrag UKGM, and by the Leibniz Graduate School EIDIS. H.-D.K. is supported by the European Commission (FP7 project FLUPHARM), and M.S. by the Bundesministerium für Bildung und Forschung (FluResearchNet). Work in the A.G.-S. laboratories is partly supported by CRIP (Center for Research on Influenza Pathogenesis), an NIAID-funded Center of Excellence for Influenza Research and Surveillance (CEIRS, contract number HHSN272201400008C), and by NIAD HHSN 272201000054C contract and U19AI083025 grant.

Received: August 12, 2014
Revised: October 24, 2014
Accepted: January 5, 2015
Published: February 19, 2015

REFERENCES

Barber, M.R., Aldridge, J.R., Jr., Webster, R.G., and Magor, K.E. (2010). Association of RIG-I with innate immunity of ducks to influenza. Proc. Natl. Acad. Sci. USA *107*, 5913–5918.

Baron, J., Tarnow, C., Mayoli-Nüssle, D., Schilling, E., Meyer, D., Hammami, M., Schwalm, F., Steinmetzer, T., Guan, Y., Garten, W., et al. (2013). Matriptase, HAT, and TMPRSS2 activate the hemagglutinin of H9N2 influenza A viruses. J. Virol. *87*, 1811–1820.

Baum, A., Sachidanandam, R., and García-Sastre, A. (2010). Preference of RIG-I for short viral RNA molecules in infected cells revealed by next-generation sequencing. Proc. Natl. Acad. Sci. USA *107*, 16303–16308.

Cauldwell, A.V., Moncorgé, O., and Barclay, W.S. (2013). Unstable polymerase-nucleoprotein interaction is not responsible for avian influenza virus polymerase restriction in human cells. J. Virol. *87*, 1278–1284.

Cauldwell, A.V., Long, J.S., Moncorgé, O., and Barclay, W.S. (2014). Viral determinants of influenza A virus host range. J. Gen. Virol. *95*, 1193–1210.

Foeglein, A., Loucaides, E.M., Mura, M., Wise, H.M., Barclay, W.S., and Digard, P. (2011). Influence of PB2 host-range determinants on the intranuclear mobility of the influenza A virus polymerase. J. Gen. Virol. *92*, 1650–1661.

Gabriel, G., Klingel, K., Otte, A., Thiele, S., Hudjetz, B., Arman-Kalcek, G., Sauter, M., Shmidt, T., Rother, F., Baumgarte, S., et al. (2011). Differential use of importin-alpha isoforms governs cell tropism and host adaptation of influenza virus. Nat. Comm. *2*, 156.

Gack, M.U. (2014). Mechanisms of RIG-I-like receptor activation and manipulation by viral pathogens. J. Virol. *88*, 5213–5216.

Graef, K.M., Vreede, F.T., Lau, Y.F., McCall, A.W., Carr, S.M., Subbarao, K., and Fodor, E. (2010). The PB2 subunit of the influenza virus RNA polymerase affects virulence by interacting with the mitochondrial antiviral signaling protein and inhibiting expression of beta interferon. J. Virol. *84*, 8433–8445.

Habjan, M., Andersson, I., Klingström, J., Schümann, M., Martin, A., Zimmermann, P., Wagner, V., Pichlmair, A., Schneider, U., Mühlberger, E., et al. (2008). Processing of genome 5′ termini as a strategy of negative-strand RNA viruses to avoid RIG-I-dependent interferon induction. PLoS ONE *3*, e2032.

Hale, B.G. (2014). Conformational plasticity of the influenza A virus NS1 protein. J. Gen. Virol. *95*, 2099–2105.

Hatta, M., Gao, P., Halfmann, P., and Kawaoka, Y. (2001). Molecular basis for high virulence of Hong Kong H5N1 influenza A viruses. Science *293*, 1840–1842.

Hornung, V., Ellegast, J., Kim, S., Brzózka, K., Jung, A., Kato, H., Poeck, H., Akira, S., Conzelmann, K.K., Schlee, M., et al. (2006). 5′-Triphosphate RNA is the ligand for RIG-I. Science *314*, 994–997.

Hudjetz, B., and Gabriel, G. (2012). Human-like PB2 627K influenza virus polymerase activity is regulated by importin-α1 and -α7. PLoS Pathog. *8*, e1002488.

Iwai, A., Shiozaki, T., Kawai, T., Akira, S., Kawaoka, Y., Takada, A., Kida, H., and Miyazaki, T. (2010). Influenza A virus polymerase inhibits type I interferon induction by binding to interferon beta promoter stimulator 1. J. Biol. Chem. *285*, 32064–32074.

Jagger, B.W., Wise, H.M., Kash, J.C., Walters, K.A., Wills, N.M., Xiao, Y.L., Dunfee, R.L., Schwartzman, L.M., Ozinsky, A., Bell, G.L., et al. (2012). An overlapping protein-coding region in influenza A virus segment 3 modulates the host response. Science *337*, 199–204.

Killip, M.J., Smith, M., Jackson, D., and Randall, R.E. (2014). Activation of the interferon induction cascade by influenza a viruses requires viral RNA synthesis and nuclear export. J. Virol. *88*, 3942–3952.

Kim, J.K., Negovetich, N.J., Forrest, H.L., and Webster, R.G. (2009). Ducks: the "Trojan horses" of H5N1 influenza. Influenza Other Respi. Viruses *3*, 121–128.

Klenk, H.D. (2014). Influenza viruses en route from birds to man. Cell Host Microbe *15*, 653–654.

Kowalinski, E., Lunardi, T., McCarthy, A.A., Louber, J., Brunel, J., Grigorov, B., Gerlier, D., and Cusack, S. (2011). Structural basis for the activation of innate immune pattern-recognition receptor RIG-I by viral RNA. Cell *147*, 423–435.

Labadie, K., Dos Santos Afonso, E., Rameix-Welti, M.A., van der Werf, S., and Naffakh, N. (2007). Host-range determinants on the PB2 protein of influenza A viruses control the interaction between the viral polymerase and nucleoprotein in human cells. Virology *362*, 271–282.

Li, W., Chen, H., Sutton, T., Obadan, A., and Perez, D.R. (2014). Interactions between the influenza A virus RNA polymerase components and retinoic acid-inducible gene I. J. Virol. *88*, 10432–10447.

Liedmann, S., Hrincius, E.R., Guy, C., Anhlan, D., Dierkes, R., Carter, R., Wu, G., Staeheli, P., Green, D.R., Wolff, T., et al. (2014). Viral suppressors of the RIG-I-mediated interferon response are pre-packaged in influenza virions. Nat. Comm. *5*, 5645.

Livak, K.J., and Schmittgen, T.D. (2001). Analysis of relative gene expression data using real-time quantitative PCR and the 2(-Delta Delta C(T)) Method. Methods *25*, 402–408.

Long, L., Deng, Y., Yao, F., Guan, D., Feng, Y., Jiang, H., Li, X., Hu, P., Lu, X., Wang, H., et al. (2014). Recruitment of phosphatase PP2A by RACK1 adaptor protein deactivates transcription factor IRF3 and limits type I interferon signaling. Immunity *40*, 515–529.

Manz, B., Brunotte, L., Reuther, P., and Schwemmle, M. (2012). Adaptive mutations in NEP compensate for defective H5N1 RNA replication in cultured human cells. Nat. Comm. *3*, 802.

Mänz, B., Schwemmle, M., and Brunotte, L. (2013). Adaptation of avian influenza A virus polymerase in mammals to overcome the host species barrier. J. Virol. *87*, 7200–7209.

Marcus, P.I., Rojek, J.M., and Sekellick, M.J. (2005). Interferon induction and/or production and its suppression by influenza A viruses. J. Virol. *79*, 2880–2890.

Massin, P., van der Werf, S., and Naffakh, N. (2001). Residue 627 of PB2 is a determinant of cold sensitivity in RNA replication of avian influenza viruses. J. Virol. *75*, 5398–5404.

Mehle, A., and Doudna, J.A. (2008). An inhibitory activity in human cells restricts the function of an avian-like influenza virus polymerase. Cell Host Microbe *4*, 111–122.

Mehle, A., and Doudna, J.A. (2009). Adaptive strategies of the influenza virus polymerase for replication in humans. Proc. Natl. Acad. Sci. USA *106*, 21312–21316.

Naffakh, N., Massin, P., Escriou, N., Crescenzo-Chaigne, B., and van der Werf, S. (2000). Genetic analysis of the compatibility between polymerase proteins from human and avian strains of influenza A viruses. J. Gen. Virol. *81*, 1283–1291.

Neumann, G., Watanabe, T., and Kawaoka, Y. (2000). Plasmid-driven formation of influenza virus-like particles. J. Virol. *74*, 547–551.

Ng, A.K., Chan, W.H., Choi, S.T., Lam, M.K., Lau, K.F., Chan, P.K., Au, S.W., Fodor, E., and Shaw, P.C. (2012). Influenza polymerase activity correlates with the strength of interaction between nucleoprotein and PB2 through the host-specific residue K/E627. PLoS ONE *7*, e36415.

Österlund, P., Strengell, M., Sarin, L.P., Poranen, M.M., Fagerlund, R., Melén, K., and Julkunen, I. (2012). Incoming influenza A virus evades early host recognition, while influenza B virus induces interferon expression directly upon entry. J. Virol. *86*, 11183–11193.

Paterson, D., te Velthuis, A.J., Vreede, F.T., and Fodor, E. (2014). Host restriction of influenza virus polymerase activity by PB2 627E is diminished on short viral templates in a nucleoprotein-independent manner. J. Virol. *88*, 339–344.

Pérez-Cidoncha, M., Killip, M.J., Oliveros, J.C., Asensio, V.J., Fernández, Y., Bengoechea, J.A., Randall, R.E., and Ortín, J. (2014). An unbiased genetic screen reveals the polygenic nature of the influenza virus anti-interferon response. J. Virol. *88*, 4632–4646.

Pichlmair, A., Schulz, O., Tan, C.P., Näslund, T.I., Liljeström, P., Weber, F., and Reis e Sousa, C. (2006). RIG-I-mediated antiviral responses to single-stranded RNA bearing 5′-phosphates. Science *314*, 997–1001.

Rameix-Welti, M.A., Tomoiu, A., Dos Santos Afonso, E., van der Werf, S., and Naffakh, N. (2009). Avian Influenza A virus polymerase association with nucleoprotein, but not polymerase assembly, is impaired in human cells during the course of infection. J. Virol. *83*, 1320–1331.

Rawling, D.C., and Pyle, A.M. (2014). Parts, assembly and operation of the RIG-I family of motors. Curr. Opin. Struct. Biol. *25*, 25–33.

Resa-Infante, P., Jorba, N., Zamarreño, N., Fernández, Y., Juárez, S., and Ortín, J. (2008). The host-dependent interaction of alpha-importins with influenza PB2 polymerase subunit is required for virus RNA replication. PLoS ONE *3*, e3904.

Schlee, M. (2013). Master sensors of pathogenic RNA - RIG-I like receptors. Immunobiology *218*, 1322–1335.

Schlee, M., Roth, A., Hornung, V., Hagmann, C.A., Wimmenauer, V., Barchet, W., Coch, C., Janke, M., Mihailovic, A., Wardle, G., et al. (2009). Recognition of 5′ triphosphate by RIG-I helicase requires short blunt double-stranded RNA as contained in panhandle of negative-strand virus. Immunity *31*, 25–34.

Schmidt, A., Schwerd, T., Hamm, W., Hellmuth, J.C., Cui, S., Wenzel, M., Hoffmann, F.S., Michallet, M.C., Besch, R., Hopfner, K.P., et al. (2009). 5′-triphosphate RNA requires base-paired structures to activate antiviral signaling via RIG-I. Proc. Natl. Acad. Sci. USA *106*, 12067–12072.

Subbarao, E.K., London, W., and Murphy, B.R. (1993). A single amino acid in the PB2 gene of influenza A virus is a determinant of host range. J. Virol. *67*, 1761–1764.

Takahasi, K., Yoneyama, M., Nishihori, T., Hirai, R., Kumeta, H., Narita, R., Gale, M., Jr., Inagaki, F., and Fujita, T. (2008). Nonself RNA-sensing mechanism of RIG-I helicase and activation of antiviral immune responses. Mol. Cell *29*, 428–440.

Varga, Z.T., Ramos, I., Hai, R., Schmolke, M., García-Sastre, A., Fernandez-Sesma, A., and Palese, P. (2011). The influenza virus protein PB1-F2 inhibits the induction of type I interferon at the level of the MAVS adaptor protein. PLoS Pathog. *7*, e1002067.

Wagstaff, K.M., Sivakumaran, H., Heaton, S.M., Harrich, D., and Jans, D.A. (2012). Ivermectin is a specific inhibitor of importin α/β-mediated nuclear import able to inhibit replication of HIV-1 and dengue virus. Biochem. J. *443*, 851–856.

Weber, M., and Weber, F. (2014a). Monitoring activation of the antiviral pattern recognition receptors RIG-I and PKR by limited protease digestion and native PAGE. JoVE *89*, e51415.

Weber, M., and Weber, F. (2014b). Segmented negative-strand RNA viruses and RIG-I: divide (your genome) and rule. Curr. Opin. Microbiol. *20*, 96–102.

Weber, M., Gawanbacht, A., Habjan, M., Rang, A., Borner, C., Schmidt, A.M., Veitinger, S., Jacob, R., Devignot, S., Kochs, G., et al. (2013). Incoming RNA virus nucleocapsids containing a 5′-triphosphorylated genome activate RIG-I and antiviral signaling. Cell Host Microbe *13*, 336–346.

Wisskirchen, C., Ludersdorfer, T.H., Müller, D.A., Moritz, E., and Pavlovic, J. (2011). The cellular RNA helicase UAP56 is required for prevention of double-stranded RNA formation during influenza A virus infection. J. Virol. *85*, 8646–8655.

Wunderlich, K., Juozapaitis, M., Ranadheera, C., Kessler, U., Martin, A., Eisel, J., Beutling, U., Frank, R., and Schwemmle, M. (2011). Identification of high-affinity PB1-derived peptides with enhanced affinity to the PA protein of influenza A virus polymerase. Antimicrob. Agents Chemother. *55*, 696–702.

Yamada, S., Hatta, M., Staker, B.L., Watanabe, S., Imai, M., Shinya, K., Sakai-Tagawa, Y., Ito, M., Ozawa, M., Watanabe, T., et al. (2010). Biological and structural characterization of a host-adapting amino acid in influenza virus. PLoS Pathog. *6*, e1001034.

Yoo, J.S., Kato, H., and Fujita, T. (2014). Sensing viral invasion by RIG-I like receptors. Curr. Opin. Microbiol. *20*, 131–138.